A Cable-Driven Parallel Mechanism for the Interaction with Hemispherical Surfaces

K.H.J. Voss, V. van der Wijk, and J.L. Herder

Abstract In this paper, a device based upon a specific cable-driven parallel mechanism to interact with hemispherical surfaces is proposed and investigated. This device could be of use in, for example, the automated cleaning of glass domes. Because the cables move on the hemispherical surface, they are curved. A method is developed to calculate the inverse kinematics and the workspace of this mechanism. This method and device are applied to and evaluated for an example of a large glass dome, showing its potential for this purpose.

Keywords Cable-driven parallel mechanism • Surface interaction • Workspace • Kinematics

1 Introduction

The cleaning of glass domes, which appear in an increasing number of buildings, is a challenging task because of the difficulty in reaching the entire surface. Therefore the cleaning is very expensive, mainly because of the considerable amount of human labor involved [1]. In addition, it is a dangerous task for humans.

Automated devices for cleaning exist, but they require significant adaptations to the building and the structure of the surface, e.g. the implementation of guidance rails [2]. Some of these devices are designed for a specific dome, which makes them an expensive solution. Carts which are rolling on the surface have the problem that they need manual (and thus expensive) steering or suction tracks, which requires a vacuum pump and additional safeguards against falling.

K.H.J. Voss (✉) • V. van der Wijk • J.L. Herder
Laboratory of Mechanical Automation and Mechatronics, Faculty of Engineering Technology, University of Twente, P.O. Box 217, 7500AE Enschede, The Netherlands
e-mail: k.h.j.voss@alumnus.utwente.nl

F. Viadero and M. Ceccarelli (eds.), *New Trends in Mechanism and Machine Science*, Mechanisms and Machine Science 7, DOI 10.1007/978-94-007-4902-3_44,

In this paper a new automated device is proposed and investigated that can have an application in the cleaning of glass domes. It is based upon the concept of cable-driven parallel mechanisms (CDPMs), which are known to have a large workspace to mass ratio, to be easy to reconfigure and to be relatively cheap to produce [3, 4].

CDPMs usually consist of cables that run freely from the base to a moving platform, e.g. [5–7]. Theoretical investigations are therefore based on straight cables, e.g. [8, 9], or sagged cables when cable mass is considered, e.g. [10, 11]. For the proposed device however, the cables lie along a hemispherical surface and are therefore curved because of contact with the surface. For such a device no theory was found.

The goal of this paper is to develop and apply a method to calculate the inverse kinematics and the workspace of a CDPM with curved cables that lie on a large hemispherical surface. It also aims to evaluate the potential of this concept for the cleaning of glass domes.

Firstly, the mechanism configuration is proposed. Then a method is developed to calculate the inverse kinematics and the workspace of the mechanism. With a numerical example the concept is evaluated and the results are discussed.

2 Mechanism Configuration and Definitions

Figure 1 shows the proposed mechanism configuration on a hemispherical surface with a constant radius r. The mechanism consists of four cables that are attached to base points A_i and run along the surface towards the moving platform $B_1B_2B_3B_4$ to which they are connected. The platform is moved by lengthening or shortening the cables at the B_i. A fixed coordinate frame F with origin O_F is located at the center of the base of the hemisphere and a mobile coordinate frame M with origin O_M is fixed to the platform. Subscripts F or M indicate whether a vector is described in F or M respectively. Base points A_i are described by constant vectors $\mathbf{A_{i,F}} = \overrightarrow{O_F A_1}$ and platform points B_i are described by constant vectors $\mathbf{B_{i,M}} = \overrightarrow{O_M B_1}$. The mass m of the platform is assumed to be centered in O_M. With a cleaning head [12] on the platform, the surface could be cleaned.

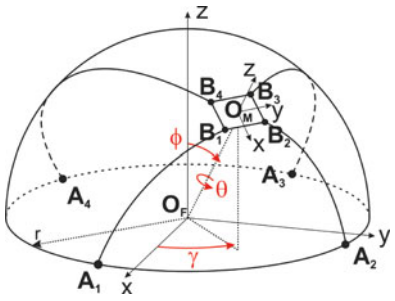

Fig. 1 Mechanism configuration

The relation between M and F can be described by first a translation of radius r along z_F, followed by consecutive rotations of θ around z_F, φ around y_F, and γ around z_F, as indicated in Fig. 1. These rotations are the DOF and they determine the platform pose $\mathbf{x} = [\theta, \varphi, \gamma]^T$. In this way θ describes the local orientation of the platform while φ and γ describe its position on the hemispherical surface.

An arbitrary vector $\mathbf{Q_M}$ in M can be described in F by

$$\mathbf{Q_F} = \mathbf{R_z}(\gamma)\,\mathbf{R_y}(\phi)\,\mathbf{R_z}(\theta)\left(\mathbf{Q_M} + [0,0,r]^T\right) = \mathbf{R}(\theta,\phi,\gamma)\left(\mathbf{Q_M} + [0,0,r]^T\right) \quad (1)$$

$$\mathbf{Q_M} = \mathbf{R}^{-1}\mathbf{Q_F} - [0,0,r]^T = \mathbf{R}^T\mathbf{Q_F} - [0,0,r]^T \quad (2)$$

in which $\mathbf{R}_y$ and $\mathbf{R}_z$ are elementary 3×3 rotation matrices.

Since the cables are in contact with the surface, friction can have a significant influence. However, engineering solutions are available with which this friction is low. With the actuated winches located at B_i the cables will not have to slide along the surface in the direction along the cables. For sideward motion, when the cables are surrounded by a series of small and soft beads that roll along the surface, also friction in this direction is minimized.

The mass of the cables can also have an effect on the mechanism. However, for simplicity and because part of the cable mass is carried by the surface, the cables are assumed massless. Together, the assumptions of friction- and massless cables imply that each cable is always connected from A_i to B_i along the shortest possible path. This path lies on a circumferential arc of the hemisphere, i.e. an arc with a radius equal to r. This attribute will be used in the next section.

3 Method

Figure 2 shows a cable lying on its circumferential arc, i.e. the shortest path on the hemisphere from A_i to B_i. The cable length length L_i is calculated with

$$L_i = 2r\alpha = 2r\,a\sin\left(\frac{\|\mathbf{A_{i,F}} - \mathbf{B_{i,F}}\|}{2r}\right) = g_i(\mathbf{x}) \quad (3)$$

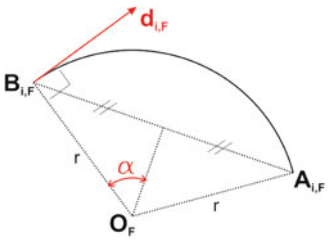

Fig. 2 A cable on its circumferential arc

All $\mathbf{B_{i,F}}$ can be calculated with Eq. 1 as a function of a pose $\mathbf{x}$. All $\mathbf{A_{i,F}}$ are known constant vectors. Then $\mathbf{g(x)} = [g_1(\mathbf{x}), g_2(\mathbf{x}), g_3(\mathbf{x}), g_4(\mathbf{x})]^T$ is the inverse kinematics function that maps the DOF of the platform to the cable lengths. Using $\mathbf{g(x)}$, the platform can be moved to a desired pose on the dome by controlling the cable lengths.

The poses the mechanism can reach is defined as the workspace for which the cable tension forces can make a static equilibrium on the platform. The resulting forces and torques $\mathbf{f_M}$ on the platform in *M* due to cable tensions $\mathbf{t}$ can be calculated with [13]:

$$\mathbf{W_M t} = \begin{bmatrix} \mathbf{u_{1,M}} & \cdots & \mathbf{u_{4,M}} \\ \mathbf{B_{1,M}} \times \mathbf{u_{1,M}} & \cdots & \mathbf{B_{4,M}} \times \mathbf{u_{4,M}} \end{bmatrix} \begin{bmatrix} T_1 \\ T_2 \\ T_3 \\ T_4 \end{bmatrix} = \begin{bmatrix} F_{x,M} \\ F_{y,M} \\ F_{z,M} \\ M_{xx,M} \\ M_{yy,M} \\ M_{zz,M} \end{bmatrix} = \mathbf{f_M} \tag{4}$$

Where wrench matrix $\mathbf{W_M}$ contains direction vectors $\mathbf{u_i}$ for the cable tensions. Because the mechanism has curved cables, the direction of the cable tension described in *F* is along vector $\mathbf{d_{i,F}}$ in Fig. 2, which is tangential to the circumferential arc. $\mathbf{d_{i,F}}$ is the cross product of $\mathbf{B_{i,F}}$ with the normal vector of the plane in which A_i, B_i and the circumferential arc lie and is given by Eq. 5. When the $\mathbf{d_{i,F}}$ are normalized and rotated to *M* with Eq. 6, the $\mathbf{u_{i,M}}$ of Eq. 4 are calculated.

$$\mathbf{d_{i,F}} = \mathbf{B_{i,F}} \times (\mathbf{A_{i,F}} \times \mathbf{B_{i,F}}) \tag{5}$$

$$\mathbf{u_{i,M}} = \mathbf{R^T} \frac{\mathbf{d_{i,F}}}{\|\mathbf{d_{i,F}}\|} \tag{6}$$

$F_{z,M}$, $M_{xx,M}$ and $M_{yy,M}$ do not affect the equilibrium since they are always compensated for because of surface contact. Because the mobile platform is always in contact with the surface, these are always balanced by reaction forces and torques of the surface on the mobile platform. For the equilibrium calculations therefore the reduced 3×4 wrench matrix $\mathbf{W_{M,eqlb}}$ (Eq. 7) is used. The workspace is defined as the set of poses for which Eq. 7 can be satisfied with $t_{min} < T_i < t_{max}$ for i = 1, 2, 3, 4. This test is a well-known problem in linear programming [14].

$$\mathbf{W_{M,eqlb}} = \mathbf{W_M}([1,2,6],[1,2,3,4]), \quad \mathbf{W_{M,eqlb}t} = \mathbf{f_{M,eqlb}} \tag{7}$$

$$\mathbf{W_{M,norm}} = \mathbf{W_M}([3],[1,2,3,4]), \quad \mathbf{W_{M,norm}t} = F_{z,M} \tag{8}$$

$$F_N = F_{z,M} + m(\mathbf{e_z} \cdot \mathbf{g_M}) = \mathbf{W_{M,norm}t} + m(\mathbf{e_z} \cdot \mathbf{R^T g_F}) \tag{9}$$

The normal force $F_{z,M}$ of the platform onto the surface is important for surface interaction considerations. 1×4 wrench matrix $\mathbf{W_{M,norm}}$ (Eq. 8) can be used to calculate this normal force. For the total normal force F_N on the platform, gravity forces need to be taken into account. With Eq. 9, where $\mathbf{e_z} = [0, 0, 1]^T$ and $\mathbf{g_F}$ is the vector describing the gravitational acceleration, the total normal force can be calculated.

4 Results

For the workspace analysis a numerical example is used with the parameters of Table 1 and $r = 15$ m, $m = 100$ kg and $\mathbf{g_F} = [0, 0, -9.81]$ m/s^2. Figure 3 shows a mechanism pose with force direction vectors $\mathbf{u}$, for $\mathbf{x} = [-20°, 30°, 45°]^T$.

Table 1 Coordinate vectors

	$A_{1,F}$	$A_{2,F}$	$A_{3,F}$	$A_{4,F}$	$B_{1,F}$	$B_{2,F}$	$B_{3,F}$	$B_{4,F}$
x (m)	−10.61	10.61	10.61	−10.61	−2.34	2.34	2.34	−2.34
y (m)	−10.61	−10.61	10.61	10.61	−0.18	−0.18	0.18	0.18
z (m)	0	0	0	0	−0.18	−0.18	−0.18	−0.18

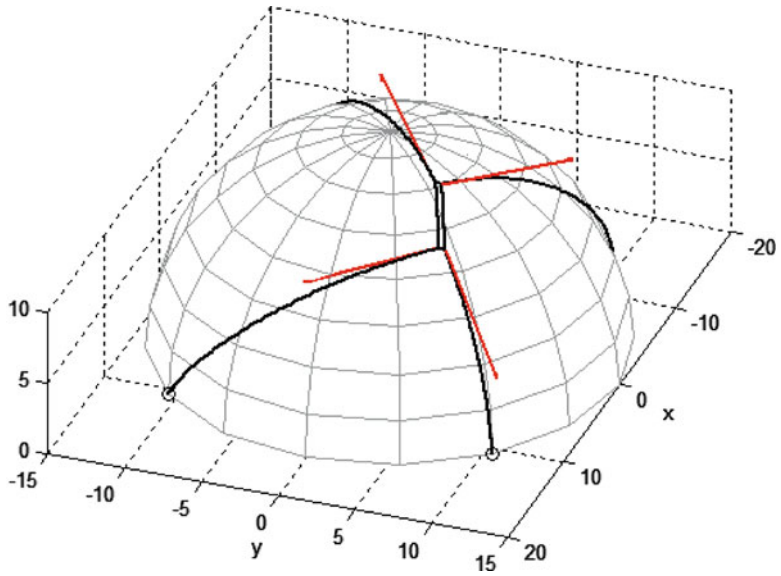

Fig. 3 A mechanism for $x = [-20°, 30°, 45°]^T$, showing the force direction vectors

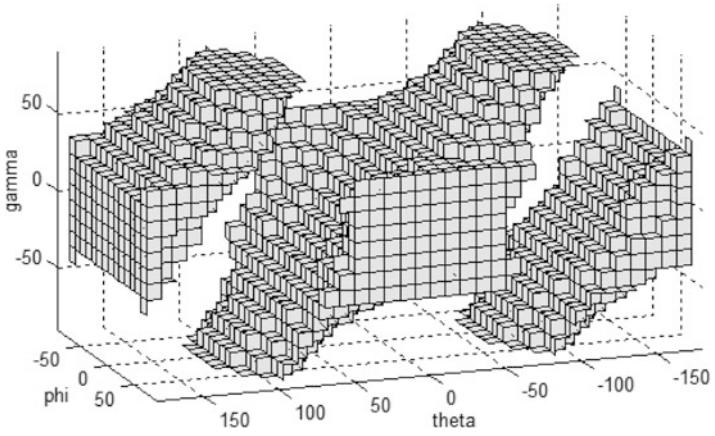

Fig. 4 Workspace for a grid of $-180° \leq \theta \leq 180°$, $-90° \leq \varphi \leq 90°$ and $-90° \leq \gamma \leq 90°$

The workspace is calculated for each pose on a predefined grid with a resolution of 5° in all DOF. $t_{min} = 100$ N, $t_{max} = 3{,}000$ N and $\mathbf{f_{M,eqlb}}$ is calculated with Eq. 10 to impose equilibrium while taking the effect of gravity into account. $\mathbf{e_x} = [1, 0, 0]^T$ and $\mathbf{e_y} = [0, 1, 0]^T$. Figure 4 shows the calculated workspace for a grid of $-180° \leq \theta \leq 180°$, $-90° \leq \varphi \leq 90°$ and $-90° \leq \gamma \leq 90°$.

$$\mathbf{f_{M,eqlb}} = \begin{bmatrix} F_{x,M} \\ F_{y,M} \\ M_{zz,M} \end{bmatrix} = - \begin{bmatrix} m\left(\mathbf{e_x} \cdot \mathbf{R^T g_F}\right) \\ m\left(\mathbf{e_y} \cdot \mathbf{R^T g_F}\right) \\ 0 \end{bmatrix} \tag{10}$$

The workspace consists of separate volumes. From a practical point of view, not all volumes are useful since they may represent an instable equilibrium. For example, consider the pose $\mathbf{x} = [180°, 0°, 0°]^T$, illustrated in Fig. 5, which is part of the workspace according to Fig. 4. Here, the cable tensions produce a normal force away from the surface. This may cause the platform to flip over. The cables also interfere with one other. Another observation is that the volumes are completely disjoint, which means that starting from a pose in the one volume, e.g. $\mathbf{x} = [0°, 0°, 0°]^T$, a pose in the other volume cannot be reached along paths where equilibrium is maintained continuously.

Figure 6 shows the workspace of Fig. 4 for the poses without interfering cables and for $\zeta = \theta + \gamma$ instead of θ.

Now it is clear that the workspace is the largest for $\zeta = 0°$, i.e. when the local orientation θ equals $-\gamma$. This is illustrated in Fig. 7. The mechanism is then able to reach the entire hemispherical surface with the exception of the areas around $\varphi = \pm 90°$ and $\gamma = \pm 90°$. If the mechanism is used for a cleaning application, these areas are easily reached and cleaned by hand.

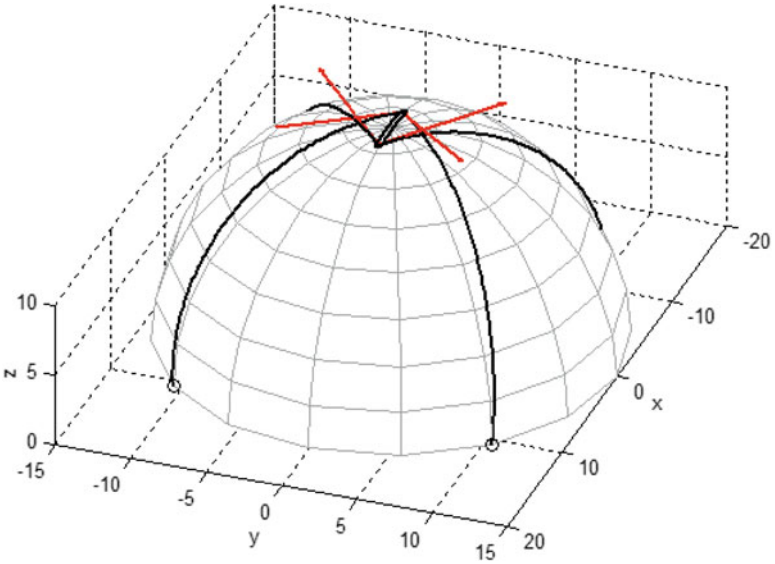

Fig. 5 The pose $x = [180°, 0°, 0°]^T$ with interfering cables

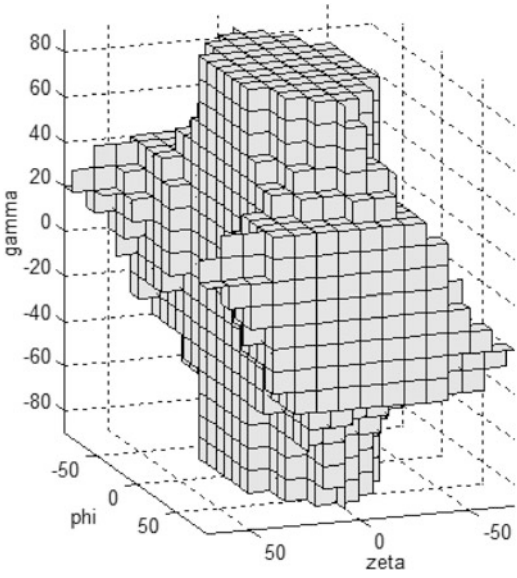

Fig. 6 Interference free workspace for $\zeta = \theta + \gamma$

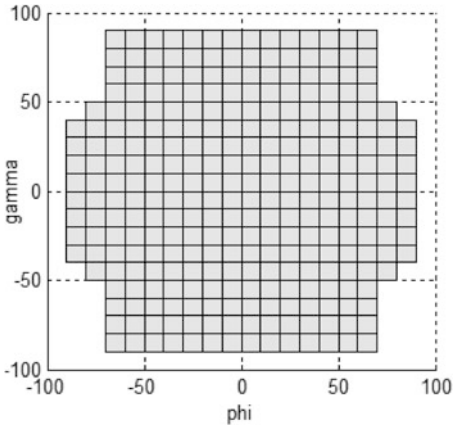

Fig. 7 The same workspace for $\zeta = 0°$

5 Discussion

The presented method is not only applicable to hemispherical surfaces, but to spherical surfaces in general and for any orientation with respect to gravity. It can be used to aid in the design of a device acting on such a surface. The idea of cables that lie on a surface can also be applied to mechanisms interacting with non-spherical surfaces, but for this the presented method needs to be extended.

The method and results of this paper are based on the assumption of massless cables. When their mass would be included, the effect would be that the cables sag down a little along the surface. For the inverse kinematics, this would mean slightly longer cable lengths. For the determination of the workspace, the change in $\mathbf{u_i}$ would be minimal, but cable tensions might become higher. The effect of cable mass and also of the remaining friction present between the cables and the surface is topic of further investigation.

For the use of the proposed mechanism as a cleaning device for glass domes, the only requirement to the building is the installment of four anchor points. The device can also be easily shared among several domes, making it a cost-effective solution.

6 Conclusion

Contrary to common CDPMs where cables run freely through space, a CDPM with cables that slide along a spherical surface has been proposed. A method has been developed to calculate the inverse kinematics and wrench matrix of this mechanism. The method was applied and with the wrench matrix the workspace was determined for a numerical example.

The results have shown that this mechanism is able to reach almost the entire hemispherical surface, while at the same time a stable equilibrium is maintained. This makes the proposed device applicable to e.g. the cleaning of glass domes.

References

1. Gambao, E., Hernando, M., Hernández, F., Pinilla, E.: Cost-effective robots for façade cleaning. In: Proceedings of the 21st ISARC, Jeju, South Korea (2004)
2. Schraft, R.D., Bräuning, U., Orlowski, T., Hornemann, M.: Automated cleaning of windows on standard facades. Automat. Constr. **9**(5–6), 489–501 (2000)
3. Merlet, J.-P.: Parallel Robots, 2nd edn, pp. 68–69. Springer, Dordrecht (2006)
4. Gouttefarde, M., Gosselin, C.: Analysis of the wrench-closure workspace of planar parallel cable-driven mechanisms. IEEE Trans. Robot. **22**(3), 434–445 (2006)
5. Kawamura, S., Choe, W., Tanaka, S., Pandian, S.R.: Development of an ultrahigh speed robot FALCON using wire drive system. In: IEEE International Conference on Robotics and Automation, vol. 1, pp. 215–220 (1995)
6. Merlet, J.-P.: Kinematics of the wire-driven parallel robot MARIONET using linear actuators. In: IEEE International Conference on Robotics and Automation, pp. 3857–3862 (2008)
7. Deschenes, J.-D., et al.: A cable-driven parallel mechanism for capturing object appearance from multiple viewpoints. In: IEEE International Conference on 3-D Digital Imaging and Modeling, no. 3, pp. 367–374 (2007)
8. Borgstrom, P.H., Jordan, B.L., Sukhatme, G.S., Batalin, M.A., Kaiser, W.J.: Rapid computation of optimally safe tension distributions for parallel cable-driven robots. IEEE Trans. Robot. **25**(6), 1271–1281 (2009)
9. Bedoustani, Y.B., Taghirad, H.D., Aref, M.M.: Dynamics analysis of a redundant parallel manipulator driven by elastic cables. In: 10th International Conference on Control, Automation, Robotics and Vision, pp. 536–542 (2008)
10. Riehl, N., Gouttefarde, M., Baradat, C., Pierrot, F.: On the determination of cable characteristics for large dimension cable-driven parallel mechanisms. In: IEEE International Conference on Robotics and Automation, pp. 4709–4714 (2010)
11. Kozak, K.: Static analysis of cable-driven manipulators with non-negligible cable mass. IEEE Trans. Robot. **22**(3), 425–433 (2006)
12. Dornier, I.: Brush cleaning head, US Patent WO 98/461121998
13. Bruckmann, T., Mikelsons, L., Brandt, T., Hiller, M., Schramm, D.: Wire Robots Part I - Kinematics, Analysis and Design, vol. 1, pp. 109–132. Parallel Manipulators – New Developments, I-Tech Education and Publishing, Vienna (2008)
14. Gouttefarde, M., Merlet, J.-P., Daney, D.: Wrench-feasible workspace of parallel cable-driven mechanisms. In: IEEE International Conference on Robotics and Automation, Roma, no 1, pp. 1492–1497 (2007)